

This is a repository copy of *Fabrication and Application of Isotopically Labelled Gold Arrays for Multiplexed Peptide Analysis*.

White Rose Research Online URL for this paper:  
<https://eprints.whiterose.ac.uk/104884/>

Version: Accepted Version

---

**Article:**

Castangia, Roberto, Hudson, Sian, Robinson, Helen et al. (3 more authors) (2016)  
Fabrication and Application of Isotopically Labelled Gold Arrays for Multiplexed Peptide  
Analysis. *Chembiochem*. ISSN 1439-7633

<https://doi.org/10.1002/cbic.201600347>

---

**Reuse**

Items deposited in White Rose Research Online are protected by copyright, with all rights reserved unless indicated otherwise. They may be downloaded and/or printed for private study, or other acts as permitted by national copyright laws. The publisher or other rights holders may allow further reproduction and re-use of the full text version. This is indicated by the licence information on the White Rose Research Online record for the item.

**Takedown**

If you consider content in White Rose Research Online to be in breach of UK law, please notify us by emailing [eprints@whiterose.ac.uk](mailto:eprints@whiterose.ac.uk) including the URL of the record and the reason for the withdrawal request.

A EUROPEAN JOURNAL

# CHEMPHYSCHEM

OF CHEMICAL PHYSICS AND PHYSICAL CHEMISTRY

## Accepted Article

**Title:** Competition between Halogen, Hydrogen and Dihydrogen Bonding in Brominated Carboranes

**Authors:** Jindrich Fanfrlik; Josef Holub; Zdenka Ruzickova; Jan Rezac; Paul Lane; Derek Wann; Drahomir Hnyk; Ales Ruzicka; Pavel Hobza

This manuscript has been accepted after peer review and the authors have elected to post their Accepted Article online prior to editing, proofing, and formal publication of the final Version of Record (VoR). This work is currently citable by using the Digital Object Identifier (DOI) given below. The VoR will be published online in Early View as soon as possible and may be different to this Accepted Article as a result of editing. Readers should obtain the VoR from the journal website shown below when it is published to ensure accuracy of information. The authors are responsible for the content of this Accepted Article.

**To be cited as:** ChemPhysChem 10.1002/cphc.201600848

**Link to VoR:** <http://dx.doi.org/10.1002/cphc.201600848>

A Journal of



[www.chemphyschem.org](http://www.chemphyschem.org)

WILEY-VCH

# Competition between Halogen, Hydrogen and Dihydrogen Bonding in Brominated Carboranes

Jindřich Fanfrlík,<sup>\*[a]</sup> Josef Holub,<sup>[b]</sup> Zdeňka Růžičková,<sup>[c]</sup> Jan Řezáč,<sup>[a]</sup> Paul D. Lane,<sup>[d],[e]</sup> Derek A. Wann,<sup>[d]</sup> Drahomír Hnyk,<sup>\*[b]</sup> Aleš Růžička<sup>\*[c]</sup> and Pavel Hobza<sup>[a],[f]</sup>

**Abstract:** Halogen bonds are a subset of noncovalent interactions with rapidly expanding applications in materials and medicinal chemistry. While halogen bonding is well known in organic compounds, it is new in the field of boron cluster chemistry. We have synthesized and crystallized carboranes containing Br atoms in two different positions, namely bound to C- and B-vertices. The Br atoms bound to the C-vertices have been found to form halogen bonds in the crystal structures. In contrast, Br atoms bound to B-vertices formed hydrogen bonds. Quantum chemical calculations have revealed that halogen bonding in carboranes can be much stronger than in organic architectures. These findings open new possibilities for applications of carboranes both in materials and medicinal chemistry.

Halogen bonds (X-bonds) are nonclassical noncovalent interactions between halogen atoms (X) and electron ( $e^-$ ) donors.<sup>[1]</sup> X-bonding belongs to the family of  $\sigma$ -hole interactions, and has received a lot of attention during the last decade.<sup>[1]</sup> Despite the first X-bond being described by Hassel as early as 1954,<sup>[2]</sup> the nature of the X-bond was only explained in 2007.<sup>[3]</sup> X-bonding is enabled by a region of partial positive charge (the so-called  $\sigma$ -hole), which is located on the top of the partially negative X atom. A  $\sigma$ -hole can be characterized by its size and magnitude ( $V_{s,max}$ ), which in turn determines the properties of the X-bond.<sup>[4]</sup> The strength of an X-bond can thus be increased by increasing the  $V_{s,max}$  value (keeping the same  $e^-$  donor). This has already been demonstrated in small model systems<sup>[5]</sup> as

well as in protein-ligand complexes.<sup>[6]</sup>

Polyhedral boron hydrides are a large group of compounds with unique properties, a wide range of applications,<sup>[7]</sup> and unusual noncovalent interactions.<sup>[8]</sup> The group includes compounds displaying 3D aromaticity and an ability to form dihydrogen bonds (HH-bonds)<sup>[9]</sup> and chalcogen bonds.<sup>[10]</sup> HH-bonds are unconventional proton-hydride H-bonds characterized by a short distance between H atoms. They generally occur between a positively charged hydrogen of a proton donor (e.g. CH, NH, OH groups) and a  $\sigma$ -bonding electron pair from an MH bond (M = electropositive atom, such as B, Al, Li). Many studies have shown the importance of HH-bonding in crystal packing and supramolecular chemistry.<sup>[11]</sup> Furthermore, it has been shown that carborane-based inhibitors interact with their biomolecular targets mainly *via* formation of HH-bonds.<sup>[12]</sup> Recently, we studied the properties of halogenated carboranes using quantum mechanics (QM) methods. These calculations showed that halogenated carboranes had large and highly positive  $\sigma$ -holes when an X atom was covalently attached to the C-vertex of a neutral carborane molecule.<sup>[13,14]</sup>

In this current study, we have synthesized the  $C_{5s}$ -symmetrical carboranes 9-Br-*closo*-1,2- $C_2B_{10}H_{11}$  (**1**) and 1,12-Br<sub>2</sub>-*closo*-1,2- $C_2B_{10}H_{10}$  (**2**), which have been characterized by NMR spectroscopy (Table S1), and using X-ray crystallography. **1** and **2** are compared to 1-Ph-2-Br-*closo*-1,2- $C_2B_{10}H_{10}$  (**3**), which was previously synthesized by Welch *et al.*<sup>[15]</sup> who also determined the crystal structure. The pairwise interactions in all three crystal structures (**1–3**) were studied using high-level QM calculations. We performed highly accurate MP2.5/CBS calculations<sup>[16]</sup> for all the binding motifs; benchmark calculations using CCSD(T)/CBS were also performed for selected interactions of **1**.

Initially, we compared the computed properties of isolated molecules. **1** has a single Br atom bound to a B-vertex, which results in a large computed dipole moment ( $\mu$ ) of 6.4 D. As a consequence, the electrostatic potential (ESP) on the Br atom was found to be highly negative. The negative ESP on the Br atom was due to the fact that it is covalently bound to an electropositive B atom. The  $V_{s,max}$  of the Br atom on **1** thus had a negative value of  $-8.8 \text{ kcal mol}^{-1}$ , which was, however, less negative than the belt around the center of the atom. The anisotropic charge distribution on the Br atom points to a relative  $\sigma$ -hole. Because the entire surface of the Br atom has negative ESP, the Br atom of **1** can only act as an electron donor when involved in, for example, H-bonding.

Molecule **2** contains two differently bonded Br atoms. One is bound to a C-vertex and the second to a B-vertex. The  $V_{s,max}$  of the Br atom bound to the B-vertex has a negative value ( $-5.0 \text{ kcal mol}^{-1}$ ), as was the case for **1**. However, the Br atom bound to the C-vertex has a positive ESP ( $V_{s,max} = 31.3 \text{ kcal mol}^{-1}$ ). Moreover, even the belt around the Br atom was found to have a positive ESP. This is a very large  $V_{s,max}$  value, particularly if we consider that the  $V_{s,max}$  values for bromobenzene and pentafluoro-bromobenzene are 11.2 and 29.7  $\text{kcal mol}^{-1}$ ,

- [a] Dr. J. Fanfrlík[+], Dr. J. Řezáč, Prof. P. Hobza  
Institute of Organic Chemistry and Biochemistry,  
Academy of Sciences of the Czech Republic v.v.i.  
Flemingovo nám. 2, 16610 Prague 6, Czech Republic  
E-mail: fanfrlik@uochb.cas.cz
- [b] Dr. J. Holub[+], Dr. D. Hnyk  
Institute of Inorganic Chemistry  
Academy of Sciences of the Czech Republic, v.v.i.  
250 68 Řež u Prahy, Czech Republic  
E-mail: hnyk@iic.cas.cz
- [c] Dr. Z Růžičková[+], Prof. A. Růžička  
University of Pardubice  
Studentská 573, Pardubice, Czech Republic  
E-mail: ales.ruzicka@upce.cz
- [d] Dr. P. D. Lane, Dr. D. A. Wann  
Department of Chemistry  
University of York  
Heslington, York, YO10 5DD, UK
- [e] Dr. P. D. Lane (current address)  
School of Engineering and Physical Sciences  
Heriot-Watt University  
Riccarton, Edinburgh, EH14 4AS, UK
- [f] Prof. P. Hobza  
Regional Center of Advanced Technologies and Materials,  
Department of Physical Chemistry  
Palacký University, 77146 Olomouc, Czech Republic

[+] These authors have contributed equally to this work.  
Supporting information for this article can be found under  
<http://dx.doi.org/XXXXXXXXXX>.

respectively.<sup>[13]</sup> **2** could thus form both H- and X-bonds (an H-bond exclusively *via* the Br bound to B-vertex, and an X-bond exclusively *via* the Br atom bound to C-vertex). **2** has a smaller computed  $\mu$  value (5.2 D) than **1**.

**3** has a single Br atom bound to a C-vertex. The ESP of the Br atom of **3** is less positive than the ESP of the corresponding Br atom on **2**. The  $V_{s,max}$  value is smaller than that for **2** but is still highly positive (25.7 kcal mol<sup>-1</sup>). The ESP of the belt of the Br atom is, however, negative. The single Br atom of **3** could thus form both X- and H-bonds simultaneously. The calculated  $\mu$  value for **3** is about 4.8 D, which is in acceptable agreement with the experimental value of 4.1 D.<sup>[17]</sup> The experimental  $\mu$  value for **3** has been explained by its vector analysis.<sup>[17]</sup> The value of  $\mu$  for **3** was thus smaller than that those calculated for **1** and **2**.

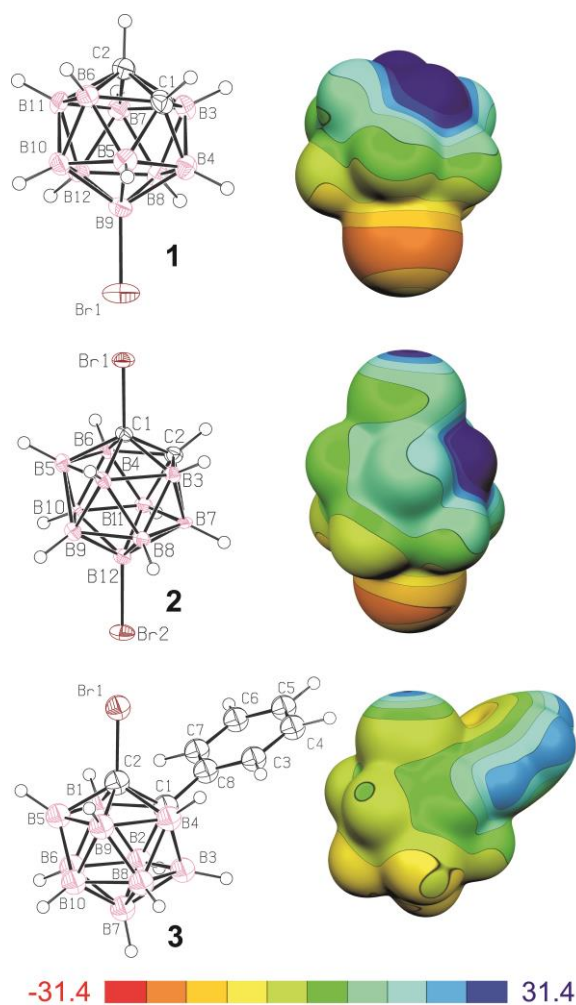


**Figure 1.** ORTEP views and computed electrostatic potential (ESP) on 0.001 a.u. molecular surface at the HF/cc-pVDZ level. Color range of ESP in kcal mol<sup>-1</sup>.

Secondly, we solved the crystal structures of **1** and **2**. In the crystal structure of **1**, two independent molecules were found in the unit cell. The shortest skeletal interatomic distance is attributed to the C–C moiety, which also corresponds to the

supramolecular connectivity of one B–Br fragment with two C–H groups building thus the global array (Figure 1). In the previously reported but incomplete (hydrogen atoms not determined) crystal structure of **2**,<sup>[18]</sup> the positions of the skeletal C atoms were based on simple comparison of interatomic distances between all pairs of skeletal atoms (the shortest separation was attributed to the HC–CBr fragment). We have now entirely redetermined the structure of **2** at lower temperature using state-of-the-art methods; the connectivity in the supramolecular architecture of **2** is distinguished on the basis of connectivity between the E–Br (E = C or B atoms) and appropriate E–H moieties from the neighboring carborane. This approach takes into the account the difference in Allen electronegativities<sup>[19]</sup> of elements and groups involved; *e.g.*  $\Delta\chi_{Allen}(B-H) = -0.249$ , while the differences for C–H, C–Br and B–Br groups are +0.244, –0.141 and –0.634, respectively

Comparing Allen electronegativities also confirms the widely accepted fact the B–Br...H–C hydrogen bond is highly preferred ( $\Delta\chi_{Allen} = 0.878$ ). In general, the supramolecular architecture of 2Br–C<sub>2</sub>B<sub>10</sub> is best described as a helix-like linear chain of two units interconnected by the B–Br...H–C interactions. Moreover, each level of the helix is interconnected with another one of the same helix or neighboring helix by an C–Br...H–B X-bond or HH-bond. Because of substitutional/static disordering of the skeletal atoms within the structure of **2**, averaging of atomic positions occurs. This leads to the shortest interatomic distance being between BrC–BH fragments. On the other hand, the elongation of the B–Br separation in comparison to the C–Br one by approximately 0.1 Å corresponds to the appropriate bond distance in **1**.

Thirdly, we analyzed interactions in the crystal structures. The crystal packing and the binding motifs are shown in Figure 2. The interaction energy ( $\Delta E$ ) values are summarized in Table 1. Each Br atom of **1** made two H-bonds with C–H vertices of other molecules. These B–Br...H–C H-bonds were 2.7 Å long and had  $\Delta E$  of –6.0 and –5.7 kcal mol<sup>-1</sup>. The strength of the H-bond could be caused by the large partial negative charges on the Br atom and large  $\mu$ .

The crystal packing of **2** clearly demonstrates the two different interactions that the Br atoms can make. The Br atom bound to B-vertex forms well-known B–Br...H–C H-bonds, while the Br atom bound to the C-vertex is shown to form novel C–Br...H–B X-bonds. The H-bonding in **2** is weaker than in that for **1**, which might be due to the smaller  $\mu$  and sub-optimal arrangement. In this case, C–H interacts with the less negative top part of X atom, and not with the highly negative belt. Even though the  $V_{s,max}$  for **2** was highly positive,  $\Delta E$  of the X-bond was only –2.9 kcal mol<sup>-1</sup>. These observations could also be due to the suboptimal arrangement of the X-bond.<sup>[20]</sup> The optimal X-bond arrangement is linear, while the C–Br...H angle in this architecture is 166°. Moreover, the e<sup>-</sup>-deficient carborane cage is likely to be a bad e<sup>-</sup> donor. Interestingly, there are five binding motifs in the crystal structure with strengths that lie within a narrow range of 0.5 kcal mol<sup>-1</sup>. This could lead to significant competition between the different interactions during the growth of the supramolecular structure.

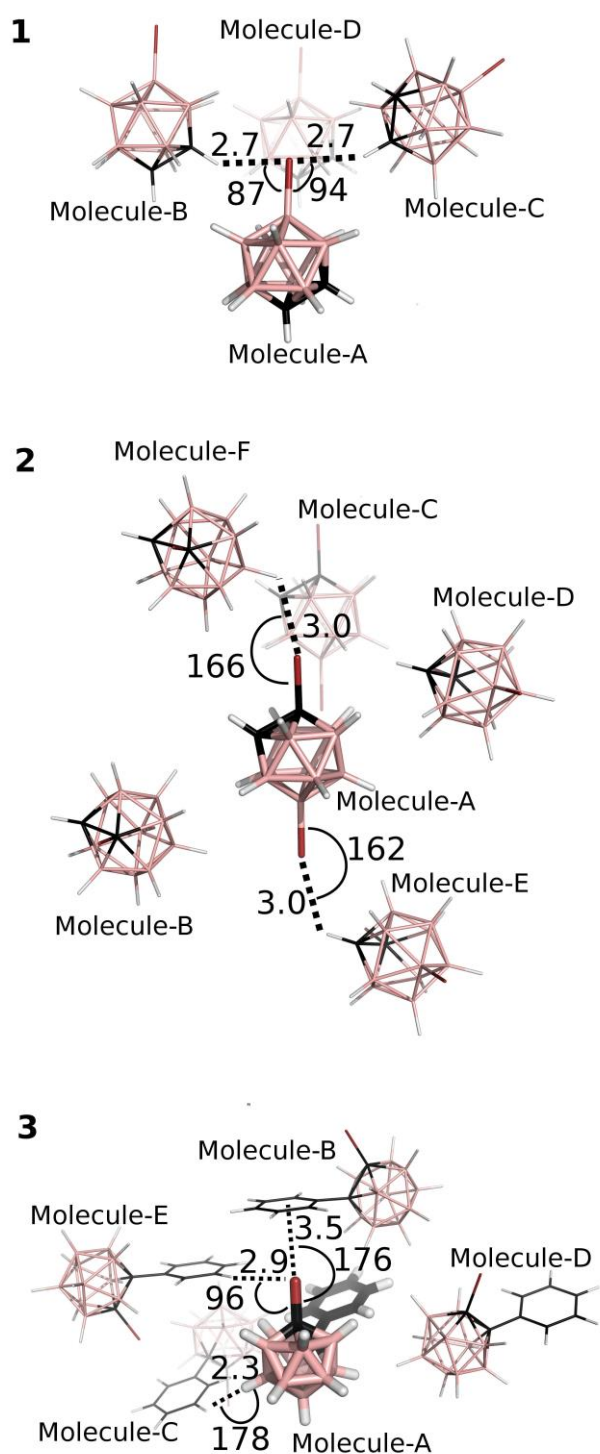


**Figure 2.** The most stable interaction motifs from the studied crystals. Distances in Å. Angles in degrees. The color coding is as follows: red, bromine; black, carbon; pink, boron; white, hydrogen.

The crystal packing in the structure of **3**<sup>[15]</sup> is dominated by the X-bond between the Br and the Ph ring.  $\Delta E$  of  $-6.7$  kcal mol<sup>-1</sup> in **3** was the strongest  $\Delta E$  of all three compounds. It should be however noticed that there is an additional interaction in the A-B motif of **3**: a HH-bond with an H...H distance of 2.4 Å. Similar

HH-bonds can be found in the A-C binding motif (see Figure 2), which is characterized by two symmetrical HH-bonds formed between B-H and the H atoms of the Ph rings. That A-C HH-bond was shorter (2.3 Å) and thus probably stronger. Taking half the  $\Delta E$  value of the A-C binding motif could thus be considered as an upper limit for the strength of the additional interactions in the A-B motif. The estimated  $\Delta E$  of the isolated X-bond would thus be about  $-4$  kcal mol<sup>-1</sup>, which is close to the  $\Delta E$  value calculated for the 1...benzene complex ( $-3.3$  kcal mol<sup>-1</sup>).<sup>[14]</sup> The reported X-bond can, however, be considered a particularly strong X-bond, when compared with X-bonds for organic compounds. For example,  $\Delta E$  for the benzene...BrCH<sub>3</sub> and benzene...BrCF<sub>3</sub> complexes were reported to be about  $-1.8$  and  $-3.1$  kcal mol<sup>-1</sup>, respectively.<sup>[21,22]</sup> This comparison confirms the remarkable ability of heteroboron clusters to form very strong  $\sigma$ -hole interactions.<sup>[13,14]</sup> Another exceptionally strong  $\sigma$ -hole binding motif has been reported in the crystal structure of 12-Ph-*closo*-1-SB<sub>11</sub>H<sub>10</sub>, where the chalcogen binding motif had  $\Delta E$  of  $-8.6$  kcal mol<sup>-1</sup>.<sup>[10]</sup>

**Table 1.** Interaction energies in kcal mol<sup>-1</sup>.

Motif	Interaction	MP2.5/CCSD(T)
	9-Br- <i>closo</i> -1,2-C <sub>2</sub> B <sub>10</sub> H <sub>11</sub>	
A-B	H-bond	-5.85/-6.00
A-C	H-bond	-5.55/-5.69
A-D	Stacking	-2.32
	1,12-Br <sub>2</sub> - <i>closo</i> -1,2-C <sub>2</sub> B <sub>10</sub> H <sub>10</sub>	
A-B	Stacking	-3.37
A-C	Stacking (Parallel displaced)	-3.32
A-D	Stacking	-3.22
A-E	H-bond	-3.12
A-F	X-bond	-2.91
	1-Ph-2-Br- <i>closo</i> -1,2-C <sub>2</sub> B <sub>10</sub> H <sub>10</sub>	
A-B	X-bond	-6.73
A-C	HH-bond	-5.09
A-D	Stacking	-3.52
A-E	H-bond	-2.82

To sum up, we have compared the crystal packing of carboranes containing Br atoms attached to different cage atoms. When Br is bound to C-vertices X-bonds are formed, while Br bound to B-vertices formed H-bonds. QM analyses revealed the strength of the X-bonds in carboranes. The knowledge about noncovalent interactions of halogenated carboranes can be employed in various applications. Besides crystal engineering, it can be used, for example, to increase binding affinity of carborane-based inhibitors towards their biomolecular targets. Furthermore, X-bonds might play an important role in chemical reactions that involve halogenated carboranes. The knowledge obtained from this study might, therefore, also be useful when designing novel synthetic paths.

## Experimental Section

See Supporting Information for full experimental details.



The synthetic procedure for **1** and **2** was based on the gradual bromination of *o*-carborane. At first, the *o*-carborane reacted with Br<sub>2</sub> and AlBr<sub>3</sub> and **1** was obtained. Subsequently, **1** underwent magnesylation-based bromination with C<sub>2</sub>H<sub>5</sub>MgBr and Br<sub>2</sub> to obtain **2**. For further details see Reference 23.

As compounds **1** and **2** have not so far been characterized by using NMR spectroscopy, the principal experimental structural tool in boron cluster chemistry, we have performed such spectroscopic studies to determine the architectures of **1** and **2** unambiguously. The corresponding shielding tensors were also computed.

Crystals of **1** and **2** were grown by slow evaporation of hexane solutions. Crystallographic data for structural analysis have been deposited with the Cambridge Crystallographic Data Centre (1459071 and 1459072 for **1** and **2**, respectively).

Quantum mechanical (QM) calculations were performed using the X-ray crystal structures. Hydrogen atoms of the crystal structures were optimized using the newly parameterized DFT-D3/BLYP/DZVP method.  $\Delta E$  values were obtained using MP2.5 and CCSD(T) complete basis set calculations. Electrostatic potentials were computed at HF/cc-pVDZ level. It has recently been shown that larger basis sets are not needed for this purpose.<sup>[24]</sup>

## Acknowledgements

This work was supported by research project RVO 61388963 of the Academy of Sciences of the Czech Republic. We acknowledge the financial support of the Czech Science Foundation (JF, JR, PH: P208/12/G016 and DH, JH: 15-056775). We also thank the Gilead Sciences and IOCB Research Center for financial support. DAW and PDL thank the UK National Service for Computational Chemistry Software for the provision of hardware and software. This work was supported by the Ministry of Education, Youth and Sports from the Large Infrastructures for Research, Experimental Development and Innovations project "IT4Innovations National Supercomputing Center – LM2015070" as well as from project LO1305 (PH).

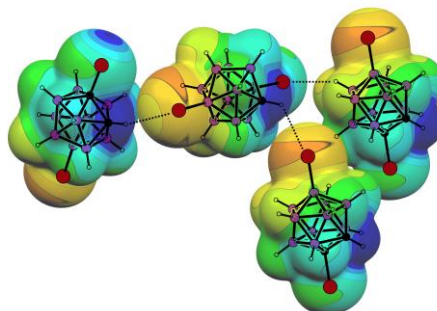
**Keywords:** carborane•sigma hole•halogen bond•bromine•X-ray crystal structure

- [1] a) P. Politzer, J. S. Murray, *ChemPhysChem* **2013**, *14*, 278-294; b) A. Bauza, T. J. Mooibroek, A. Frontera, *ChemPhysChem* **2015**, *16*, 2496-2517; c) G. Cavallo, P. Metrangolo, R. Milani, T. Pilati, A. Priimagi, G. Resnati, G. Terraneo, *Chem. Rev.* **2016**, *116*, 2478-2601; d) R. Wilcken, M. O. Zimmermann, A. Lange, A. C. Joerger, F. M. Boeckler, *J. Med. Chem.* **2013**, *56*, 1363-1388; e) M. Kolar, P. Hobza, *Chem. Rev.* **2016**, *116*, 5155-5187.
- [2] O. Hassel, J. Hvoslef, *Acta Chem. Scand.* **1954**, *8*, 873.
- [3] T. Clark, M. Hennemann, J. S. Murray, P. Politzer, *J. Mol. Model.* **2007**, *13*, 291-296.
- [4] M. Kolar, J. Hostas, P. Hobza, *Phys. Chem. Chem. Phys.* **2014**, *16*, 9987-9996; **2015**, *17*, 23279-23280.
- [5] K. E. Riley, J. S. Murray, J. Fanfrlík, J. Rezac, R. J. Sola, M. C. Concha, F. M. Ramos, P. Politzer, *J. Mol. Model.* **2011**, *17*, 3309-3318.
- [6] a) L. A. Herdegger, B. Kuhn, B. Spinnler, L. Anselm, R., Ecabert, M. Stihle, B. Gsell, R. Thoma, J. Diez, J. Benz *et al. Angew. Chem., Int. Ed.* **2011**, *50*, 314-319; b) J. Fanfrlík, M. Kolar, M. Kamlar, D. Hurny, F. X. Ruiz, A. Cousins-Siah, A. Mitschler, J. Řezáč, E. Munusamy, M. Lepšík *et al., ACS Chem. Biol.* **8**, 2484-2492.
- [7] a) N. S. Hosmane, *CRC Press, Boron Science* **2011**; b) P. Cigler, M. Kozisek, P. Řezáčová, J. Brynda, Z. Otwinowski, J. Pokorna, J. Plešek, B. Gruner, L. Doleckova-Maresova, M. Masa, *et al., Proc. Natl. Acad. Sci. USA* **2005**, *102*, 15394-15399; c) J. Brynda, P. Mader, V. Šicha, M. Fábry, K. Poncová, M. Bakardiev, B. Grüner, P. Cigler, P. Řezáčová, *Angew. Chem. Int. Ed.* **2013**, *52*, 13760-13763.
- [8] R. Sedlak, J. Fanfrlík, A. Pecina, D. Hnyk, P. Hobza, M. Lepšík, in *Boron: The Fifth Element*, Springer International Publishing, **2015**, *20*, 219-239.
- [9] J. Fanfrlík, M. Lepšík, D. Horinek, Z. Havlas, P. Hobza, *ChemPhysChem* **2006**, *7*, 1100-1105.
- [10] J. Fanfrlík, A. Páda, Z. Padělková, A. Pecina, J. Macháček, M. Lepšík, J. Holub, A. Růžička, D. Hnyk, P. Hobza, *Angew. Chem. Int. Ed.* **2014**, *53*, 10139-10142.
- [11] a) J. P. Campbell, J.-W. Hwang, V. G. Young, R. B. Von Dreele, C. J. Cramer, W. L. Gladfelter, *J. Am. Chem. Soc.* **1998**, *120*, 12875-12876; b) D. G. Gusev, A. J. Lough, R. H. Morris, *J. Am. Chem. Soc.* **1998**, *120*, 13138-13147.
- [12] a) J. Fanfrlík, M. Lepšík, D. Horinek, Z. Havlas, P. Hobza, *Chem. Phys. Chem.* **2006**, *7*, 1100-1105; b) A. Pecina, M. Lepšík, J. Řezáč, J. Brynda, P. Mader, P. Rezacova, P. Hobza, J. Fanfrlík, *J. Phys. Chem. B* **2013**, *117*, 16069-16104.
- [13] R. Lo, J. Fanfrlík, M. Lepšík, P. Hobza, *Phys. Chem. Chem. Phys.* **2015**, *17*, 20814-20821.
- [14] A. Pecina, M. Lepšík, D. Hnyk, P. Hobza, J. Fanfrlík, *J. Phys. Chem. A* **2015**, *119*, 1388-1395.
- [15] T. D. McGrath, A. Welch, *Acta Crystallogr. C* **1995**, *51*, 649-651.
- [16] M. Pitoňák, P. Neogrady, J. Cerný, S. Grimme, P. Hobza, *ChemPhysChem* **2009**, *10*, 282-289.
- [17] D. Hnyk, V. Všeťečka, L. Drož, *J. Mol. Struct.* **2010**, *978*, 246-249.
- [18] V. Subrtova, A. Linek, C. Novak, *Collect. Czech. Chem. Commun.* **1975**, *40*, 2005-2011.
- [19] A. C. Leland, *J. Am. Chem. Soc.* **1989**, *111*, 9003-9014.
- [20] K. E. Riley, J. S. Murray, P. Politzer, M. C. Concha, P. Hobza, *J. Chem. Theor. Comput.* **2009**, *5*, 155-163.
- [21] A. Bauza, D. Quinonero, P. M. Deya, A. Frontera, *Cryst. Eng. Commun.* **2013**, *15*, 3137-3144.
- [22] J. Řezáč, K. E. Riley, P. Hobza, *J. Chem. Theor. Comput.* **2012**, *8*, 4285-4292.
- [23] J. Plešek, T. Hanslík, *Collect. Czech. Chem. Commun.* **1973**, *38*, 335-337.
- [24] K. E. Riley, K.-A. Tran, P. Lane, J. S. Murray, P. Politzer, *J. Comput. Sci.* **2016**, DOI: 10.1016/j.joca.2016.03.010.

## Entry for the Table of Contents

## COMMUNICATION

Substituted carboranes can contain Br atoms in two positions, namely bound to C- and B-vertices. When Br atoms are bound to C-vertices C–Br···H–B halogen bonds can be formed in the crystal structure. This is in contrast to Br atoms bound to B-vertices where B–Br···H–C hydrogen bonds are observed.



*Jindřich Fanfrlík,\* Josef Holub, Zdeňka Růžičková, Jan Řezáč, Paul D. Lane, Derek A. Wann, Drahomír Hnyk,\* Aleš Růžička\* and Pavel Hobza*

**Page No. – Page No.**

**Competition between Halogen, Hydrogen and Dihydrogen Bonding in Brominated Carboranes**

Accepted Manuscript